FINAL

Send Orders for Reprints to reprints@benthamscience.ae

Current Alzheimer Research, 2016, *13*, 000-000

Eigenanatomy on Fractional Anisotropy Imaging Provides White Matter Anatomical Features Discriminating Between Alzheimer's Disease and Late Onset Bipolar Disorder

Ariadna Besga[1,2,3,*], Darya Chyzhyk[5,8], Itxaso González-Ortega[1,2,4], Alexandre Savio[5,7], Borja Ayerdi[5,9], Jon Echeveste[6], Manuel Graña[5,7] and Ana González-Pinto[1,2,3]

[1]*Department of Psychiatry, University Hospital of Alava-Santiago, Vitoria, Spain;* [2]*Centre for Biomedical Research Network on Mental Health (CIBERSAM), Spain;* [3]*School of Medicine, University of the Basque Country, Vitoria, Spain;* [4]*School of Psychology, University of the Basque Country, San Sebastián, Spain;* [5]*Computational Intelligence Group (GIC), University of the Basque Country (UPV/EHU), San Sebastián, Spain;* [6]*Magnetic Resonance Imaging Department, Osatek-Vitoria;* [7]*ENGINE project, Wroclaw Technological University, Poland;* [8]*CISE Department, Unuversity of Florida, Gainesville, USA;* [9]*ACPySS, San Sebastian, Spain*

Ariadna Besga

Abstract: ***Background:*** Late Onset Bipolar Disorder (LOBD) is the arousal of Bipolar Disorder (BD) at old age (>60) without any previous history of disorders. LOBD is often difficult to distinguish from degenerative dementias, such as Alzheimer Disease (AD), due to comorbidities and common cognitive symptoms. Moreover, LOBD prevalence is increasing due to population aging. Biomarkers extracted from blood plasma are not discriminant because both pathologies share pathophysiological features related to neuroinflammation, therefore we look for anatomical features highly correlated with blood biomarkers that allow accurate diagnosis prediction. This may shed some light on the basic biological mechanisms leading to one or another disease. Moreover, accurate diagnosis is needed to select the best personalized treatment. ***Objective:*** We look for white matter features which are correlated with blood plasma biomarkers (inflammatory and neurotrophic) discriminating LOBD from AD. ***Materials:*** A sample of healthy controls (HC) (n=19), AD patients (n=35), and BD patients (n=24) has been recruited at the Alava University Hospital. Plasma biomarkers have been obtained at recruitment time. Diffusion weighted (DWI) magnetic resonance imaging (MRI) are obtained for each subject. ***Methods:*** DWI is preprocessed to obtain diffusion tensor imaging (DTI) data, which is reduced to fractional anisotropy (FA) data. In the selection phase, eigenanatomy finds FA eigenvolumes maximally correlated with plasma biomarkers by partial sparse canonical correlation analysis (PSCCAN). In the analysis phase, we take the eigenvolume projection coefficients as the classification features, carrying out cross-validation of support vector machine (SVM) to obtain discrimination power of each biomarker effects. The John Hopkins Universtiy white matter atlas is used to provide anatomical localizations of the detected feature clusters. ***Results:*** Classification results show that one specific biomarker of oxidative stress (malondialdehyde MDA) gives the best classification performance (accuracy 85%, F-score 86%, sensitivity, and specificity 87%,) in the discrimination of AD and LOBD. Discriminating features appear to be localized in the posterior limb of the internal capsule and superior corona radiata. ***Conclusion:*** It is feasible to support contrast diagnosis among LOBD and AD by means of predictive classifiers based on eigenanatomy features computed from FA imaging correlated to plasma biomarkers. In addition, white matter eigenanatomy localizations offer some new avenues to assess the differential pathophysiology of LOBD and AD.

Keywords: ????????????

INTRODUCTION

Bipolar disorder (BD) is a chronic mood disorder associated with cognitive, affective and functional impairment, often appearing at youth (age around 20 years), or even earlier [1], which has been considered as a risk factor for developing dementia [2]. Dementia syndrome arising as a result of a history of bipolarity does not correspond to the criteria of Alzheimer's disease (AD) [3]. However, late onset (i.e. age>60 years) BD (LOBD) [4] may be difficult to differentiate from behavioral impairment associated with Alzheimer's disease (AD), because they share overlapping symptoms and neuropathology, including cognitive impairment, emotional disturbances, neuroinflammation, excitotoxicity and upregulated brain metabolism [5, 6]. LOBD challenges the established viewpoint considering that AD and BD are distinct and unrelated clinical entities. Recent works [7, 8, 44-47], have been addressing the question from the point of view of computer aided diagnosis (CAD) systems based on imaging data. In spite of the good classification performances, results lack interpretability in terms of the anatomical localization of

*Address correspondence to this author at the Department of Psychiatry, University Hospital of Alava-Santiago, Vitoria, Spain; Centre for Biomedical Research Network on Mental Health (CIBERSAM), Spain and School of Medicine, University of the Basque Country, Vitoria, Spain;
E-mail: ariadna.besgabasterra@osakidetza.net

1567-2050/16 $58.00+.00

the effects. Also, they are unrelated to other potential disease biomarkers.

Inflammation and oxidative stress have been found as common pathopshysiological processes underlying AD [9-11], and BD [12-16], as well as many other neuropsychological illness, such as depression and mania [17-20]. These neurological disorders seem to be epigenetically linked to decreased transcriptional activity. It has been observed in both BD and AD patients that the frontal cortex exhibits an altered epigenetic regulation related to neuroinflammation, synaptic integrity and neuroprotection, and that oxidative stress contributes to the pathogenesis of both diseases through similar mechanisms [21]. The question addressed in this paper is whether there are common or differential pathophysiological effects revealed by correlation with plasma biomarkers, and their potential localization in the white matter structures.

Eigenanatomy [22, 23] is a sparse dimensional reduction procedure, which enhances detection power and interpretability by computing correlation with *a priori* relevant variables. Unlike principal component analysis (PCA) and independent component analysis (ICA), which have a global support, in eigenanatomy procedures the sparseness constraint implies that effects are localized in compact clusters. In this regard it is similar to sparse PCA. Moreover, eigenanatomy is a canonical correlation analysis (CCA), searching for projection directions with the maximal Pearson's correlation between the eigenvectors and some *a priori* relevant variables, subject to a sparseness constraint, hence it is a sparse CCA (SCCA). The approach also allows to introduce smoothness and cluster size conditions, such that the spurious small detections are removed. Eigenanatomy has been successfully applied to longitudinal cortical change detection [22, 24] , validation of a new cognitive scale [25], multimodal medical image analysis [26], and parcellation of functional imaging based on *a priori* region labeling.

Our study looks for the localization of white matter effects correlated with biomarkers applying an eigenanatomy feature extraction. Predictive CAD systems have been proposed to improve the diagnostic accuracy complementing the neuropsychological assessments carried out by expert clinicians [8, 22-25]. Accurate diagnosis is crucial to mitigate negative effects of inappropriate treatments. The classification performance achieved by machine learning based computer aided diagnosis (CAD) on eigenanatomy projection coefficients is used as a *post hoc* analysis that measures the detection power for each blood biomarker.

MATERIAL AND METHODS

The overall process is composed of selection and analysis phases. The selection phase corresponds to the eigenanatomy algorithm, which looks for sparse pseudo-eigenvectors of the fractional anisotropy (FA) volumes most correlated with the each blood biomarker. The region localizations take the form of sparse eigenvolumes, thus each subject FA volume can be expressed as a linear combination of them. The analysis phase is carried out as a classification experiment where the features are the coefficients of the linear combination, i.e. the projections of the subject FA volume onto each eigenvolume. The classification performance thus provides the discrimination power of each blood biomarker as a measure of their biomarker detection power. Therefore, classification and eigenanatomy analysis are independent processes, so that no circularity effect is incurred. Also, blood biomarkers cannot be included as classification feature because they have been used for selection. Performing the eigenanatomy over all the data we are working on the assumption that all data lie in the same subspace, which is a natural assumption. It can be argued that we are in a very subtle way using information about the test data in the training. However, besides the computational cost, performing eigenanatomy per each cross-validation folder will be a very noisy process due to the small sample size. Summarizing, the process carried out is as follows: (a) DWI data is preprocessed and converted to FA volumes, (b) eigenanatomy takes the FA volumes and each blood biomarker values, producing a collection sparse eigenvolumes and the projection coefficients, (c) the class information and the projection coefficients enter classification cross-validation experiments. Finally, (d) we examine the anatomical localization of the FA eigenvolumes clusters to report relevant findings.

SUBJECTS

Patients included in the present study were referred to the psychiatric unit at Alava University Hospital, Vitoria, from its catchment recruitment area for the clinical assessment of memory complaints. All patients were living in the community. Ninety-five elderly subjects were included in the present study. Table **1** presents demographic details of the cohort. The BD group fulfills the DSM IV criteria and the AD group fulfills the NINDS-ADRDA criteria for probable AD. Subjects with psychiatric disorders (i.e. major depression) or other conditions (i.e. brain tumors) were not considered for this study. The exclusion criteria were ongoing infections, fever, allergies, or the presence of other serious medical conditions (autoimmune, cardiac, pulmonary, endocrine, and chronic infectious diseases and neoplasms). Neither the patients nor the healthy control subjects were receiving immunosuppressive drugs or vaccinations for at least 6 months prior to inclusion in the study or anti-inflammatory analgesics the 2 days prior to the extraction of the blood sample. The ethics committee of the Alava University Hospital, Spain has approved this study. All patients gave their written consent to participate in the study, which was conducted according to the provisions of the Helsinki declaration. After written informed consent was obtained, venous blood samples (10 mL) were collected from the volunteers, after which the mood scales and cognitive tests were performed. Healthy volunteers with an MMSE score greater than 26 were recruited from the community through advertisements, nonrelated members of the patient's families and caregiver's relatives.

Image Acquisition

MRI scanning was performed on a 1.5 Tesla scanner (Magnetom Avanto, Siemens). Diffusion weighted imaging (DWI) sequence parameters were as follows: slice thickness = 5mm, 19 slices, TR=2700ms, TE=88ms, matrix 120/100, 3 averages, b=1000 and 30 gradient directions.

Table 1. Demographic data (mean and standard deviation for each group).

	HC	AD	BD
M/F	15 / 11	20 / 17	9 / 23
Age	72.81 ± 8.70	78.70 ± 5.86	68.88 ± 8.61
Education (0-5)	3.92 ± 1.14	3.33 ± 1.00	3.29 ± 1.14

Image Preprocessing

DWI images have been processed using FMRIB software library (FSL)[1] tools as follows: First, the brain extraction and eddy current correction procedure were realized using FSL's BET and eddy currents functions. Second, a diffusion tensor imaging (DTI) volume was created fitting a diffusion tensor model at each voxel. In DTI, diffusion is characterized by the eigenvalues of the three principal diffusion directions, denoted $(\lambda_1, \lambda_2, \lambda_3)$, Fractional anisotropy (FA) is computed as the ratio:

$$FA = \sqrt{\frac{1}{2}} \frac{\sqrt{(\lambda_1-\lambda_2)^2+(\lambda_1-\lambda_3)^2+(\lambda_2-\lambda_3)^2}}{\sqrt{\lambda_1^2+\lambda_2^2+\lambda_3^2}}.$$

FA values range between 0 and 1. The FSL DTIFIT tool has been used to compute the FA volume. Then, each FA volume was registered to the standard space FMRIB58_FA template. We did not perform spatial smoothing. Finally, FA mask [27] is created as the union of the individual masks obtained by applying a threshold FA > 0.60, to eliminate voxels which are not pure white matter. This FA mask contains 96.045 voxels. It is applied to each volume to extract the input data for eigenanatomy analysis.

Biological Markers (BIO)

We selected biological markers for analysis based on the on their relevance to BD and AD in the literature, i.e. studies on inflammation [9-13, 28]. After extracting plasma from blood samples, inflammatory cytokines Interleukins 1 and 6 (IL-1, IL-6) and Tumor Necrosis Factor (TNFα) were determined by enzyme immunoassay (EIA). Oxido nitrosative parameters (nitrites and malondialdehyde (MDA)) were also analyzed in plasma samples. Cytokine levels were measured by EIA using reagents in kit form for TNFα (cat. 589201), Interleukin-1β (cat. 583311) (IL1β) and Interleukin 6 (cat. 501030) (IL6) from Cayman Chemical Europe, Tallinn, Estonia. Plasma levels of TNFα, IL1β and IL6 were measured in a 96-well plate and read at 405 nm following manufacturer's instructions. Nitrites (NO^-_2), the final and stable product of nitric oxide, were measured using the Griess method, where samples are incubated in acidic solution with sulfanilamide and N-(1-naphthyl) ethylenediamine dihydrochloride (NEDA). The nitrites are converted into a pink compound that is measured photometrically at 540nm (Synergy 2, Biotek). Lipid peroxidation, the final product of the reaction of oxidonitrosative molecules with lipidic components of cells, was determined by Thiobarbituric Acid Reactive Substances (TBARS) assay (Cayman Chemical Europe, Tallinn, Estonia), based on the reaction of malondialdehyde (MDA) and thiobarbituric acid (TBA) under high temperature (95 ºC) and acidic conditions. The MDA-TBA adduct formed is measured colorimetrically at 530-540 nm (Synergy 2, Biotek). Plasma BDNF levels were measured using a BDNF Sandwich ELISA Kit, according to the manufacturer's instructions (Millipore, USA, Cat. No. CYT306). Serum NGF levels were measured with an enzyme-linked immunosorbent assay (ELISA) method according to the manufacturer's instructions, using a ChemiKineTM NGF Sandwich ELISA Kit (Millipore, USA, Cat No CYT304). All samples were assayed in duplicate. All plasma NF levels are expressed as pg/mL.

Eigenanatomy Feature Extraction

It is computed by the partial sparse canonical correlation analysis (PSCCAN) [23] provided in the ANTS open source neuroimage suite[2]. PSCCAN enriches the sparse canonical correlation analysis (SCCAN) with the ability to remove confound variables, such as age and gender. SCCAN looks for the projection maximizing the correlation between two datasets of paired observations given by matrices *X* and *Y* of dimensions $n \times p$ and $n \times q$, respectively, where n is the number of subjects in the study; in imaging studies p is the number of voxels, q is the number of measurements to be correlated with, often $p >> q$ and $p >> n$. Formally, SCCAN looks for the projection directions ψ_X and ψ_Y maximizing the Pearson's correlation after the whitening transform of the datasets, i.e.

$$x^*, y^* = \arg\max_{\psi_X, \psi_Y} \frac{\psi_X^T \Sigma_{X_w Y_w} \psi_Y}{\|\psi_X\| \|\psi_y\|}, \quad (1)$$

subject to sparseness constraints on the image eigenvectors $\|\psi_X\|_1 < s$, where $\|.\|_1$ denotes the $\|.\|_1$ norm, and s is the sparseness level, $\Sigma_{X_w Y_w} = X_w^T Y_w$ is the correlation matrix of the datasets after whitening, i.e. $X_w = X\Sigma_{XX}^{1/2}$ and $Y_w = Y\Sigma_{YY}^{1/2}$. PSCCAN considers also the confound variables in matrix Z of dimensions $n \times q'$, seeking the optimal

[1] http://fsl.fmrib.ox.ac.uk/fsl/fslwiki/

[2] http://picsl.upenn.edu/software/ants/

correlation after removing the effect of the confounding variables, i.e.

$$x^*, y^* = \arg\max_{\psi_X, \psi_Y} \frac{\psi_X^T \Sigma^{\setminus Z}_{X_w Y_w} \psi_Y}{\|\psi_X\| \|\psi_Y\|}, \quad (2)$$

where $\Sigma^{\setminus Z}_{X_w Y_w}$ is the variance-covariance matrix of the whitened residuals of the data after removing the confounding variables, $X_w = X\left(\Sigma^{\setminus Z}_{XX}\right)^{-1/2}$ and $Y_w = Y\left(\Sigma^{\setminus Z}_{YY}\right)^{-1/2}$. The residual covariance is computed as $\Sigma^{\setminus Z}_{X_w Y_w} = X^T Y - X^T Z_w Z_w^T Y$. Optimization of equation (2) is achieved by a gradient descent algorithm including a soft-max sparseness regularization at each step [23]. We only consider confound variables in relation with the imaging data contained in X. In our study, the Y matrix is composed of the values corresponding to one biomarker, hence we perform independent localizations for each; the confounding variables in Z are age and gender. The projection coefficients of the images into PSCCAN pseudo-eigenvectors are used as feature vectors for classification. The computation of PSCCAN pseudo-eigenvectors does not use class information. It can be assumed as a class independent data transformation, hence the entire process has no circularity because selection (i.e. eigenanatomy) is independent of analysis (i.e. classification). Therefore PSCCAN can be performed once for all cross-validation experiment. In the experiments we have set to 12 the number of sparse pseudo-eigenvectors, and sparseness ratio is set to s=0.1, after a heuristic exploration of the localization results obtained with several setting of these parameters.

Support Vector Machines (SVM)

Support Vector Machines (SVM) have become a sort of standard classifier for the neuroscience community [29-31], owing to a number of theoretical and computational merits [32], and to very successful implementations, such as the one provided in Matlab used in this study. In brief, SVM builds a supervised two-class classifier that separating training data samples with the maximal margin hyperplane achieving maximal generalization to new unseen data samples. The hyperplane discrimination function is defined by a set of support vectors, often localized at the boundaries between classes. The kernel trick allows define a linear discriminant in a high dimensional space, effectively obtaining a non-linear discriminant function when the data is not linearly separable. Training of SVM classifier is achieved by quadratic programming, minimizing the norm of the discriminating hyperplane parameters, subject to classification error constraints. Linear SVM have two advantages: (a) It does not require kernel parameters model selection, thus introduces no bias in the training process due to fortunate model selection, which often is tricky, (b) Allows to focus on the relative detection power associated to the features proposed, not in the optimal classifier, assuming that feature performance ranking will be invariant to the classifiers. Nevertheless, at reviewer's request and for the sake of completeness we report also results with radial basis function RBF SVMs.

Experiments

In order to evaluate the detection power of the FA pseudo-eigenvectors computed by PSCCAN maximally correlated with each biological marker, we perform 10-fold cross-validation of SVM classifiers over the datasets feature vectors obtained from projecting the FA volumes on them for each possible contrast of classes: HC vs. AD, HC vs. LOBD, AD vs. LOBD, and HC vs. AD+LOBD. In a 10-fold cross-validation approach the dataset is partitioned in 10 folds, each fold is used as the test set for the classifier build from the remaining nine folds. Performance results reported are the average values of the test performance obtained on each folder. No model selection is needed for the linear SVM. Model selection by grid search for the RBF SVM was carried out on a bootstrapped sample from the training dataset in each cross-validation fold, due to the small sample size.

Classification Performance Measures

To quantify the results we measured: (a) accuracy ((TP +TN)/N); (b) specificity (TN/(FP +TN)); (c) sensitivity (TP/(TP +FN)) and (d) F-score score is the harmonic mean of precision and sensitivity (2TP/(2TP +FP+FN)), where TP is the number of true positives: number of AD or BD patient volumes correctly classified; TN is the number of true negatives: number of control volumes correctly classified; FP is the number of false positives: number of class 1 classified as class 0; FN is the number of false negatives: number of class 0 classified as class 1.

RESULTS

Classification Results

Classification performance results are presented in Table **2** providing the accuracy, F-score, sensitivity, and specificity for each feature set corresponding to the coefficients of the optimal sparse eigenvectors correlated with the biomarker values. We provide the results for linear SVM and the best RBF SVM results. It is easy to assess that there is a significant improvement (t-test, $p<0.001$) of non-linear SVM at the cost of careful model search. However, these results do not change the relative order of blood biomarkers, hence for our purposes linear SVM provides the same information as non-linear SVM. Best discrimination of AD vs. LOBD is achieved on the feature vectors extracted from MDA, this result is statistically significant (F test computed over of all paired results per biomarker, $p<0.01$) for all performance measures. This result is the best overall, achieving more than 85% average accuracy. In independent experiments using biomarker values as classification features the accuracy in the AD vs. LOBD classification achieved was 71% and 61% for the linear and RBF SVM, respectively. Therefore, eigenanatomy greatly boosts the discrimination power. Regarding HC vs. AD, both MDA and IL6 provide the best features, a t-test computed over their paired results shows no significant difference between them ($p>0.1$). We think that features providing performance results below 70% are too weak to attribute them discrimination power. Discrimination of joint AD and LOBD from HC is very weakly achieved, maybe due to the SVM sensitivity to unbalanced datasets, pointing to the lack of a common pathophysiological source. Another

Table 2. Classification cross-validation average results for the PSCCAN coefficients maximally correlated to each plasma biomarker. Columns: L Linear SVM, RBF best SVM-RBF result obtained after model search for the RBF width, enclosed in brackets.

		Accuracy		F score		Sensitivity		Specificity	
		L	RBF	L	RBF	L	RBF	L	RBF
MDA	HC vs. AD	76.6	81.4	65.0	72.4	65.0	71.7	83.3	84.4
	AD vs. LOBD	78.3	85.3	80.9	86.7	80.8	87.3	81.6	87.4
	HC vs. D+LOBD	67.1	76.3	52.2	57.7	65.0	70.7	69.3	73.0
	HC vs. LOBD	58.0	66.8	33.3	40.1	35.0	39.6	81.6	85.4
BDNF	HC vs. AD	68.6	74.7	59.0	61.7	70.0	75.2	72.5	77.4
	AD vs. LOBD	69.6	76.7	72.1	77.9	70.0	74.2	78.3	84.1
	HC vs. DAD+LOBD	60.5	70.1	46.2	51.5	70.0	75.8	63.3	67.5
	HC vs. LOBD	49.5	60.4	54.6	58.2	70.0	73.8	43.3	58.6
NOx	HC vs. AD	65.7	72.3	55.2	59.7	65.0	68.9	71.6	76.3
	AD vs. LOBD	66.3	73.3	66.9	72.2	63.3	67.4	80.0	86.1
	HC vs. AD+LOBD	65.8	71.3	49.7	58.2	60.0	62.0	71.6	75.5
	HC vs. LOBD	56.0	65.6	52.0	59.7	65.0	71.4	56.6	61.6
Glu	HC vs. AD	69.0	76.7	58.0	61.6	70.0	75.3	75.8	81.3
	AD vs. LOBD	74.6	81.1	77.3	85.3	79.2	83.4	75.0	81.1
	HC vs. AD+LOBD	69.1	78.7	45.3	51.0	55.0	61.3	76.6	83.1
	HC vs. LOBD	58.5	67.1	40.3	45.2	50.0	53.2	76.6	81.6
IL1β	HC vs. AD	66.6	72.9	55.6	61.3	65.0	69.8	72.5	76.0
	AD vs. LOBD	71.3	79.1	73.7	78.4	71.7	76.4	76.6	80.8
	HC vs. AD+LOBD	64.3	70.4	45.5	50.3	65.0	70.3	66.6	70.5
	HC vs. LOBD	54.5	63.2	48.0	54.4	65.0	70.3	63.3	70.6
IL6	HC vs. AD	75.3	80.7	66.6	73.0	70.0	74.1	83.3	87.6
	AD vs. LOBD	71.6	78.2	71.9	78.3	68.3	73.2	81.6	87.3
	HC vs. AD+LOBD	69.3	76.4	47.0	52.6	65.0	69.8	73.0	77.8
	HC vs. LOBD	60.5	68.9	51.6	55.3	50.0	55.6	81.6	87.4
TNFα	HC vs. AD	71.3	78.3	69.4	75.1	80.0	86.0	70.8	75.0
	AD vs. LOBD	66.0	72.5	66.7	73.3	64.2	70.3	78.3	81.8
	HC vs. AD+LOBD	63.4	70.0	45.3	50.7	65.0	69.1	66.6	70.1
	HC vs. LOBD	49.5	55.3	54.7	60.7	75.0	80.0	56.6	62.0

remarkable result is the very weak detection of LOBD vs. AD for all biomarkers.

Localization Results

Anatomical localization of the effects has been performed using the John Hopkins University ICBM-DTI-81 White Matter Labels available in the FSL neuroimage suite. Table **3** contains the localizations for the principal pseudo-eigenvectors for each biomarker. Localizations are expressed as the area percentage falling in the indicated region. The middle cerebellar peduncle contains effects from almost all pesudo-eigenvectors. For visual assessment, we provide in (Fig. **1**) the localization of the principal pseudo-eigenvector over a FA template provided in the FSL suite in the sagittal, coronal and axial middle views.

Table 3. Localization of clusters in the principal pseudo-eigenvectors. Each entry correspond to the percentage of the falling in the white matter brain area.

	MDA	BDNF	Nox	Glu	IL1β	IL6	TNFα
Posterior limb of internal capsule R	10.14			2.13		4.03	
Posterior limb of internal capsule L	5.75	3.27	7.58	4.95	3.85		
Superior corona radiata R	5.92				2.75		
Superior corona radiata L	9.48			4.33	2.17		
Middle cerebellar peduncle	5.01	5.23	6.61		4.64	6.89	4.01
Retrolenticular part of internal capsule L	2.89						
Superior longitudinal fasciculus R	2.67	2.39	2.46	2.30			
Superior longitudinal fasciculus L	2.54		4.50				
Posterior thalamic radiation (include optic radiation) R		4.76	4.01	4.49		3.95	
Posterior thalamic radiation (include optic radiation) L			3.08		3.33	3.43	
Genu of corpus callosum		3.80	2.31				5.53
Splenium of corpus callosum		3.07		10.63	3.23	13.16	15.06
Body of corpus callosum		2.52		8.05	15.48	12.78	10.60
Cerebral peduncle R		2.23			3.62		2.80
Cerebral peduncle L			2.67				3.41
Corticospinal tract L			2.79				
Sagittal stratum (include inferior longitidinal fasciculus R			2.47				
Retrolenticular part of internal capsule L			2.17		2.31		
Anterior limb of internal capsule L					2.93		

DISCUSSION

This study was designed to investigate the localization in brain white matter of effects related to plasma biomarkers by eigenanatomy analysis [22, 23] that may offer insights on the common and differential pathophysiological effects of LOOBD and AD [33-35], which may allow a more accurate diagnosis supported by computer aided diagnosis (CAD) systems on the eigenanatomy coefficients. This study was motived by the increasing prevalence of LOBD and the fact that it shares many diagnostic features with AD [4, 36-38]. To our knowledge this is the first such study analyzing a wide range of biological (inflammatory, oxido-nitrosative and neurotrophic) measures for this purpose.

Peripheral markers related to inflammation, oxidative stress, and neurotrophins have been related to clinical symptoms, cognitive decline and illness severity in BD [1, 39] as well as in AD [40]. It has been suggested that inflammation and oxidative stress do not cause AD or BD by themselves, but probably during aging they reinforce many interdependent factors related to these complex neuropsychiatric disorders [3].

In the present study, most of the classification performance results for the baseline linear SVM classifier were well below 80%, which indicates very low detection power of the pseudo-eigenvectors. The only exception are the features correlated with the oxidative stress marker MDA. Cross-validation experiments with non-linear SVM carried at the request of the reviewers did improve results significantly with the additional cost of model selection. Moreover, the relative order of the biomarkers features was not affected, so the qualitative information is the same for linear and non-linear SVM. Therefore, localizations reported in Table **3** for MDA have some additional value over the other biomarkers. The main effects are found in the posterior limb of the internal capsule, and its retrolenticular part, which are strongly related to the sensory and motor areas, probably related to the degeneration of these abilities, which maybe common to both LOBD and AD, as well as aged controls. Interesting effects are found in the Superior longitudinal fasciculus containing connections between the frontal, parietal, occipital and temporal lobes. This network has been suggested to be involved in attention and language, motor behavior and somatosensory information. Abnormalities in these tracts may be related to some of the cognitive deficits found in BD [41] and cognitive performance in AD [42]. Interestingly, MDA is not related to the corpus callosum structures, so that no effect on interhemispheric communication are detected by our approach, because other biomarkers which show some

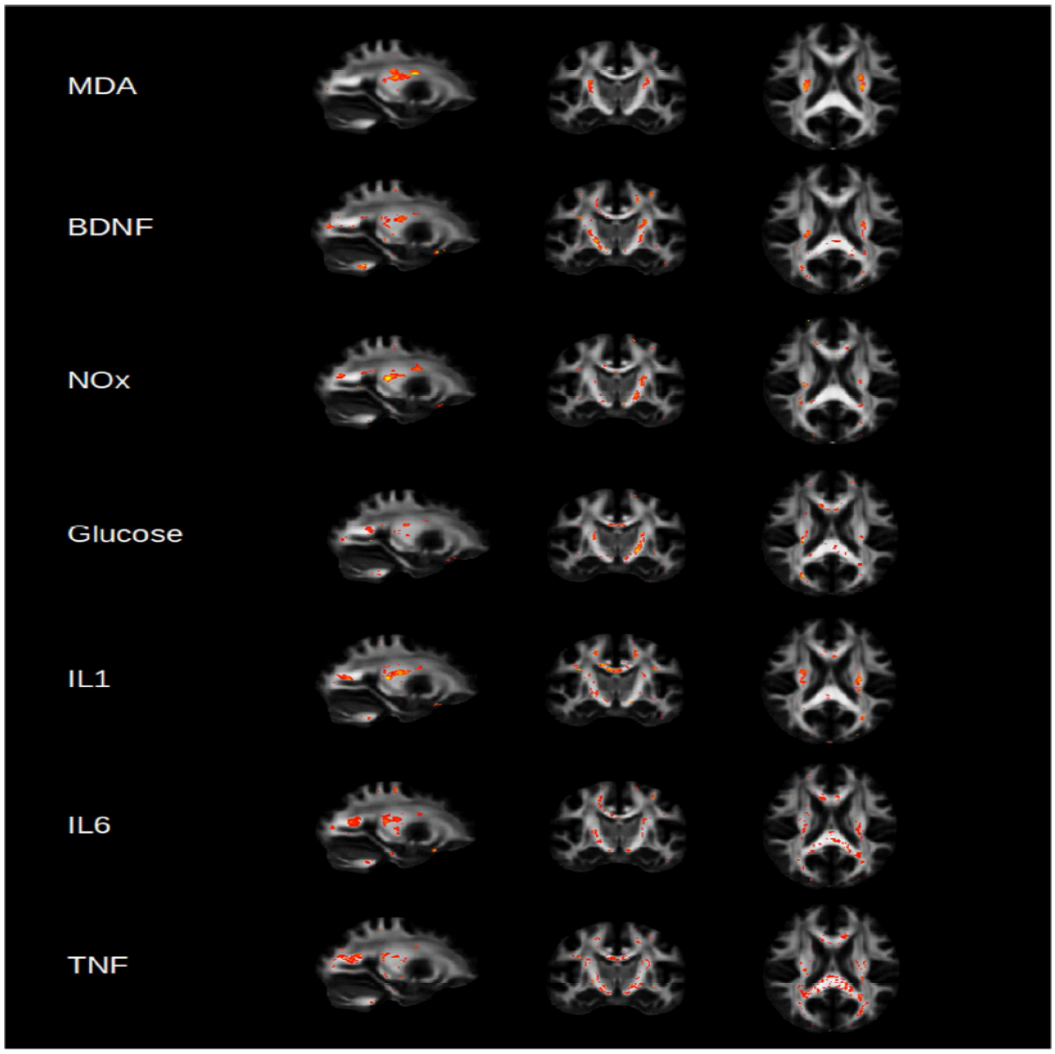

Fig. (1). Localization of the first eigenvectors maximally correlated with the corresponding biomarker visualized over the Fractional Anisotropy template, from left to right sagittal, coronal, and axial views.

localizations in the corpus callosum have very low classification performance. Finally, superior corona radiata effects are to be expected as it has been observed that aging has a definitive effect on DTI in this white matter structure [43], nevertheless it deserves further exploration in order to assess which role they play in the discrimination between LOBD and AD.

Limitations

The sample is not well balanced, there are diverse sample sizes of AD, BD and HC. The feminine BD sample is much larger.

CONCLUSION

The application of eigenanatomy to diffusion imaging correlated with plasma biomarkers has allowed to identify effects in white matter structures in agreement with the literature, providing as well a computer aided diagnostic tool aiding in the discrimination between late onset bipolar disorder and Alzheimer's disease.

Future work will be addressed to improve exploration of the parameters involved, number of eigenvectors, classifiers, sparseness parameter, as well as to use multimodal data to improve results and interpretation, including anatomical T1 weighted data.

CONFLICT OF INTEREST

The authors confirm that this article content has no conflict of interest.

ACKNOWLEDGEMENTS

This work was supported by health research funds from the local grants from the Department of Education, Linguistic Policy and Culture of the Basque Country Government 2013111162.

REFERENCES

[1] Martinez-Cengotitabengoa M, Mico JA, Arango C, Castro-Fornieles J, Graell M, Paya B, *et al.* Basal low antioxidant capacity

correlates with cognitive deficits in early onset psychosis. A 2-year follow-up study. Schizophr Res 156(1):23–29 (2014).

[2] Ng B, Camacho A, Lara DR, Brunstein MG, Pinto OC, Akiskal HS. A case series on the hypothesized connection between dementia and bipolar spectrum disorders: Bipolar type VI? J Aff Disord 107: 307-315 (2008).

[3] Forcada I, Mur M, Mora E, Vieta E, Bartras-Faz D, Portella MJ. The influence of cognitive reserve on psychosocial and neuropsychological functioning in bipolar disorder. Eur Neuropsychopharmacol 25(2): 214-222 (2015).

[4] Depp C, Jeste D. Bipolar disorder in older adults: a critical review. Bipolar Disord 6: 343-367 (2004).

[5] Rao JS, Harry GJ, Rapoport SI, Kim HW. Increased excitotoxicity and neuroinflammatory markers in postmortem frontal cortex from bipolar disorder patients. Mol Psychiatry 15: 384-392 (2010).

[6] Rao JS, Rapoport S, Kim H-W. Altered neuroinflammatory, arachidonic acid cascade and synaptic markers in postmortem Alzheimer's disease brain. Transl Psychiatry 1: 1-9 (2011)

[7] Besga A, Termenon M, Graña M, Echeveste J, Perez J, Gonzalez-Pinto A. Discovering Alzheimer's disease and bipolar disorder white matter effects building computer aided diagnostic systems on brain diffusion tensor imaging features. Neurosci Lett 520(1): 71-76 (2012).

[8] Graña M, Termenon M, Savio A, Gonzalez-Pinto A, Echeveste J, Pérez J, *et al*. Computer aided diagnosis system for Alzheimer disease using brain diffusion tensor imaging features selected by Pearson's correlation. Neurosci Lett 502(3): 225-229 (2011).

[9] Akiyama H, Barger S, Barnum S, Bradt B, Bauer J, Cole GM, *et al.* Inflammation and Alzheimer's disease. Neurobiol Aging 21(3): 383-421 (2000).

[10] Kamer AR, Craig RG, Dasanayake AP, Brys M, Glodzik-Sobanska L, de Leon MJ. Inflammation and Alzheimer's disease: Possible role of periodontal diseases. Alzheimers Dement 4(4): 242-250. (2008).

[11] Sardi F, Fassina L, Venturini L, Inguscio M, Guerriero F, Rolfo E, *et al*. Alzheimer's disease, autoimmunity and inflammation. the good, the bad and the ugly. Autoimmun Rev 11(2): 149-153 (2011).

[12] Goldstein B, Kemp D, Soczynska J, McIntyre R. Inflammation and the phenomenology, pathophysiology, comorbidity, and treatment of bipolar disorder: A systematic review of the literature. J Clin Psychiatry 70(8): 1078-1090 (2009).

[13] Lee S-Y, Chen S-L, Chang Y-H, Chen P, Huang S-Y. Inflammation's association with metabolic profiles before and after a twelve-week clinical trial in drug-naive patients with bipolar ii disorder. Plos One 8(6): e66847 (2013).

[14] Leboyer M, Soreca I, Scott J, Frye M, Henry C, Tamouza R, *et al*. Can bipolar disorder be viewed as a multi-system inflammatory disease? J Affec Disord 141(1): 1-10 (2012).

[15] Konradi C, Sillivan SE, Clay HB. Mitochondria, oligodendrocytes and inflammation in bipolar disorder: Evidence from transcriptome studies points to intriguing parallels with multiple sclerosis. Neurobiol Dis 45(1): 37-47 (2012).

[16] Bauer IE, Pascoe MC, Wollenhaupt-Aguiar B, Kapczinski F, Soares JC. Inflammatory mediators of cognitive impairment in bipolar disorder. J Psychiatr Res 56: 18-27 (2014).

[17] Castanon N, Lasselin J, Capuron L. Neuropsychiatric comorbidity in obesity: role of inflammatory processes. Neuroendocrine Sci 5: 74 (2014).

[18] Brydon L, Walker C, Wawrzyniak A, Whitehead D, Okamura H, Yajima J, *et al*. Synergistic effects of psychological and immune stressors on inflammatory cytokine and sickness responses in humans. Brain Behav Immun 23(2): 217- 224 (2009).

[19] Dickerson F, Stallings C, Origoni A, Vaughan C, Katsafanas E, Khushalani S, *et al* . A combined marker of inflammation in individuals with mania. Plos One 8(9): e73520 (2013).

[20] Singhal G, Jaehne EJ, Corrigan F, Toben C, Baune BT. Inflammasomes in neuroinflammation and changes in brain function: a focused review. Neuroendocrine Sci 8: 315 (2014).

[21] Rao JS, Keleshian VL, Klein S, Rapoport SI. Epigenetic modifications in frontal cortex from Alzheimer's disease and bipolar disorder patients. Transl Psychiatry 2: e132 (2012).

[22] Avants BB, Dhillon P, Kandel BM, Cook PA, McMillan CT, Grossman M, *et al*. Eigenanatomy Improves Detection Power for Longitudinal Cortical Change. Med Image Comput Assist Inter 15(pt. 3): 206-213 (2012).

[23] Dhillon PS, Avants BB, Ungar_L, Gee JC. Partial sparse canonical correlation analysis (pscca) for population studies in medical imaging. In Biomedical Imaging (ISBI), 9th IEEE International Symposium, pp.1132,1135, 2-5 (2012).

[24] Avants BB, Libon DJ, Rascovsky K, Boller A, McMillan CT, Massimo L, *et al.* Sparse canonical correlation analysis relates network-level atrophy to multivariate cognitive measures in a neurodegenerative population. NeuroImage 84: 698-711 (2014).

[25] Cook PA, McMillan CT, Avants BB, Peelle JE, Gee JC, Grossman M. Relating brain anatomy and cognitive ability using a multivariate multimodal framework. NeuroImage 99 : 477-486 (2014).

[26] Kandel BM, Wang DJJ, Gee JC, Avants BB, Eigenanatomy: Sparse dimensionality reduction for multi-modal medical image analysis, Methods (online first) (doi:10.1016/j.ymeth.2014.10.016).

[27] Smith SM, Jenkinson M, Johansen-Berg H, Rueckert D, Nichols TE, Mackay CE, *et al*. Tract-based spatial statistics: Voxelwise analysis of multi-subject diffusion data. NeuroImage 31: 1487-1505 (2006).

[28] García-Bueno B, Bioque M, Mac-Dowell KS, Barcones MF, Martínez-Cengotitabengoa M, Pina-Camacho L, *et al*. Proantiinflammatory dysregulation in patients with first episode of psychosis: toward an integrative inflammatory hypothesis of schizophrenia. Schizophr Bull 40(2): 376-387 (2014)

[29] Tao D, Tang X, Li X, Wu X. Asymmetric bagging and random subspace for Support Vector Machines-based relevance feedback in image retrieval. IEEE Trans. Pattern Anal Mach Intell 28(7): 1088-1099 (2006).

[30] Fung G, Stoeckel J. SVM feature selection for classification of SPECT images of Alzheimer's disease using spatial information. Knowl Inf Syst 11(2): 243-258 (2007).

[31] Burges C. A tutorial on support vector machines for pattern recognition. Data Mining Knowl Discov USA: 2(2): 167-121 (1998).

[32] Vapnik V. Statistical learning theory. Wiley- Interscience (1998).

[33] Carlino AR, Stinnett JL, Kim DR. New onset of bipolar disorder in late life. Psychosomatics 54: 94-97 (2013).

[34] Grande I, Magalhaes PV, Chendo I, Stertz L, Panizutti B, Colpo GD, *et al.* Staging bipolar disorder: clinical, biochemical, and functional correlates. Acta Psychiatr Scand 129: 437-444 (2014).

[35] Lebert F, Lys H, Haem E, Pasquier F. Dementia following bipolar disorder. Encephale 34: 606-610 (2008).

[36] Aprahamian I, Ladeira RB, Diniz BS, Forlenza OV, Nunes PV. Cognitive impairment in euthymic older adults with bipolar disorder: A controlled study using cognitive screening tests. Am J Geriatr Psychiatry 22(4): 389-397 (2014).

[37] Torrent C, Martinez-Aran A, del Mar Bonnin C, Reinares M, Daban C, Sole B, *et al.* Long-term outcome of cognitive impairment in bipolar disorder. Clin Psychiatry 73(7): e899-905. 00034 (2012).

[38] Lewandowski KE, Cohen BM, Ongur D. Evolution of neuropsychological dysfunction during the course of schizophrenia and bipolar disorder. Psychol Med 41: 225-241 (2011).

[39] Barbosa IG, Rocha NP, Huguet RB, Ferreira RA, Salgado JV, Carvalho LA, *et al.* Executive dysfunction in euthymic bipolar disorder patients and its association with plasma biomarkers. J Affec Disord 137(1- 3): 151-155. (2012).

[40] Berridge MJ. Dysregulation of neural calcium signaling in Alzheimer disease, bipolar disorder and schizophrenia. Prion 7: 2-13 (2013)

[41] van der Schot AC, Vonk R, Brouwer RM, van Baal GC, Brans RG, van Haren NE, *et al*. Genetic and environmental influences on focal brain density in bipolar disorder. Brain 133(10): 3080-3092 (2010).

[42] Sasson E, Doniger GM, Pasternak O, Tarrasch R, Assaf Y. Structural correlates of cognitive domains in normal aging with diffusion tensor imaging. Brain Struct Funct 217(2): 503-515 (2012).

[43] Bendlin BB, Fitzgerald ME, Ries ML, Xu G, Kastman EK, Thiel BW, *et al*. White Matter in Aging and Cognition: A Cross-sectional Study of Microstructure in Adults Aged Eighteen to Eighty-Three. Develop Neuropsychol 35(3): 257-277 (2010).

[44] Chyzhyk D, Graña M. Classification of Schizophrenia patients on Lattice Computing resting-state fMRI features. Neurocomputing 151 (1): 151-160 (2015).

[45] Chyzhyk D, Savio A, Graña M. Evolutionary ELM wrapper feature selection for Alzheimer's disease CAD on anatomical brain MRI. Neurocomputing 128: 73-80 (2014).

[46] Chyzhyk D. Bootstrapped Dendritic Classifiers for Alzheimer's Disease classification on MRI features. Advanced in Knowledge-Based and Intelligence Information and Engineering Systems.

Front Art Intelligence and Applications (FAIA) series, Amsterdam, NL IOS Press, Vol. 243: pp. 2251-2258 (2012).

[47] Chyzhyk D, Graña M, Öngür D, Shinn AK. Discrimination of Schizophrenia Auditory Hallucinators by Machine Learning of Resting-State Functional MRI. Int J Neural Syst 25(3): 1550007 (2015).

Received: ???????????????? **Revised: ????????????????** **Accepted: ????????????????**